

Antiferromagnetic EuTe Clusters in $\text{Ge}_{1-x}\text{Eu}_x\text{Te}$ Semiconductors

L. KILANSKI^{a,*}, M. GÓRSKA^a, M. ARCISZEWSKA^a, A. PODGÓRNI^a, R. MINIKAYEV^a,
B. BRODOWSKA^a, A. RESZKA^a, B.J. KOWALSKI^a, V.E. SLYNKO^b AND E.I. SLYNKO^b

^aInstitute of Physics, Polish Academy of Sciences, Aleja Lotnikow 32/46, PL-02668 Warsaw, Poland

^bInstitute of Materials Science Problems, Ukrainian Academy of Sciences, 5 Wilde Str., 274001 Chernovtsy, Ukraine

We present studies of structural, electrical, and magnetic properties of $\text{Ge}_{1-x}\text{Eu}_x\text{Te}$ bulk crystals with the chemical composition, x , changing from 0.020 to 0.025. The sample synthesis leads to the formation of EuTe clusters in all our samples. Moreover, the presence of $\text{Ge}_{1-x}\text{Eu}_x\text{Te}$ spinodal decompositions with broad range of chemical contents is observed even for the sample with $x = 0.020$. Spinodal decompositions show the antiferromagnetic order with the Néel temperature, T_N , equal to about 11 K, close to that for EuTe. The magnetic field dependence of the magnetization, $M(B)$, is characteristic of the presence of magnetic inclusions in the samples.

DOI: [10.12693/APhysPolA.134.950](https://doi.org/10.12693/APhysPolA.134.950)

PACS/topics: diluted magnetic semiconductors, magnetic properties, clusters

1. Introduction

Magnetic and transport properties of transition-metal-doped GeTe compounds belonging to IV–VI diluted magnetic semiconductors (DMS) have been studied during the past twenty years [1–5]. High Curie temperatures, T_C , were reported and attributed to carrier-induced ferromagnetic interactions. For $\text{Ge}_{1-x}\text{Mn}_x\text{Te}$ the highest T_C value was about 190 K [3, 4] and for $\text{Ge}_{1-x}\text{Cr}_x\text{Te}$ about 180 K [5]. There have been no systematic investigations of GeTe doped with rare-earth ions.

Previously we studied magnetic properties of Eu-codoped $\text{Ge}_{1-x}\text{Mn}_x\text{Te}$ [6] and $\text{Ge}_{1-x}\text{Cr}_x\text{Te}$ [7] with the Eu content up to 0.04. We observed Curie temperatures about 150 K for $\text{Ge}_{1-x-y}\text{Mn}_x\text{Eu}_y\text{Te}$ and 80 K for $\text{Ge}_{1-x-y}\text{Cr}_x\text{Eu}_y\text{Te}$. However, in these materials there was a strong tendency to form different types of clusters. The clusters modified significantly the properties of the materials. Similar behavior was observed before in $\text{Sn}_{1-x}\text{Eu}_x\text{Te}$, where Eu clusters were detected for x above 0.013 [8].

In the present paper we investigate magnetic interactions in GeTe crystals with the Eu content less than 0.03. We pay special attention to the problem of limited solubility of europium ions in the GeTe lattice. Our studies aim at an estimation of the limits of the Eu content in which the $\text{Ge}_{1-x}\text{Eu}_x\text{Te}$ compounds are uniform DMS.

2. Sample preparation

The studied $\text{Ge}_{1-x}\text{Eu}_x\text{Te}$ bulk crystals were grown by the modified Bridgman method. We applied the modifications of the Bridgman growth process similar to those

made by Aust and Chalmers in order to improve the structural quality of alumina crystals [9]. We modified the standard vertical Bridgman–Stockbarger technique by installing the additional heating elements in the growth furnace in order to create some radial temperature gradient in addition to the longitudinal temperature gradient in the crystallization zone. The applied modification tilted the crystallization front from the horizontal position by about 15°. This value was measured by the deviation of the normal to the end face of the cylindrical ingot from the axis of the cylinder. The applied modifications of the growth process reduced the number of crystal blocks in the as-grown ingots from a few down to a single one.

3. Basic characterization

We started the structural characterization of the as-grown $\text{Ge}_{1-x}\text{Eu}_x\text{Te}$ crystal slices from the measurements of their chemical compositions with the use of the energy dispersive X-ray fluorescence technique (EDXRF) employed to the Tracor X-ray Spectrace 5000 EDXRF spectrometer. The EDXRF data allow the calculation of the Eu content, x , with the maximum relative error not higher than 10% of the x value. The as grown ingot was cut perpendicular to the growth direction into 1.5 mm thick slices. The chemical composition of each slice was measured with the EDXRF technique. The EDXRF data analysis shows that x changed along the ingot from 0.002 to 0.03, but the cation–anion ratio along the ingot remained 50:50. For the present study we selected several samples, in which the calculated average Eu content, x , changed from 0.020 up to 0.025.

We used the high resolution X-ray diffraction method (HRXRD) for powdered $\text{Ge}_{1-x}\text{Eu}_x\text{Te}$ samples using the high resolution X'Pert MPD Pro Alpha1, Panalytical diffractometer with Cu K_{α_1} ($\lambda = 1.540598 \text{ \AA}$). All the HRXRD diffraction patterns were measured during 20 h

*corresponding author; e-mail: kilan@ifpan.edu.pl

in the 2θ range from 5 deg to 160 deg. The obtained diffraction patterns were analyzed by using the Rietveld refinement method. This procedure allowed us to determine the crystal system, the Bravais lattice, and to calculate the unit cell parameters. The selected HRXRD results for the $\text{Ge}_{1-x}\text{Eu}_x\text{Te}$ samples with $x = 0.025$ are presented in Fig. 1.

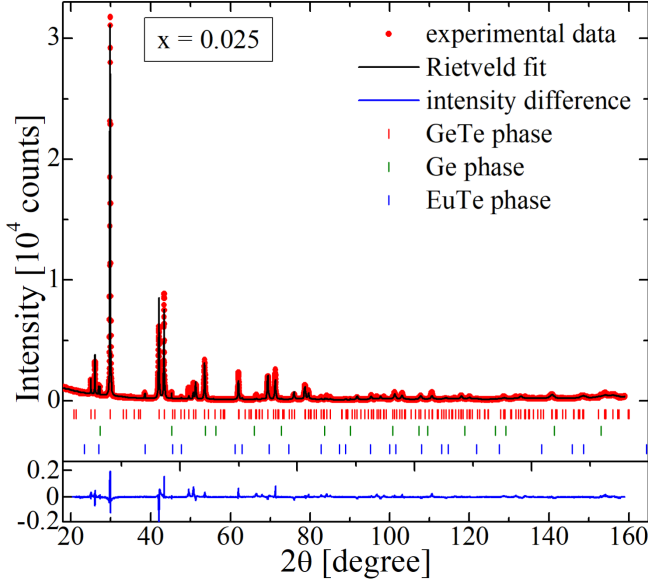


Fig. 1. Selected XRD experimental results (red points) obtained for the $\text{Ge}_{1-x}\text{Eu}_x\text{Te}$ sample $x = 0.025$. Black line represents the Rietveld fit to the experimental results. Color markers represent database data for the three phases detected for our samples. Blue line represents the difference between the experimental data and the fitted diffraction pattern.

The phase analysis of the obtained diffraction patterns showed that for all our samples we observed the presence of three phases: (i) rhombohedral NaCl structure for the main $\text{Ge}_{1-x}\text{Eu}_x\text{Te}$ phase, (ii) cubic NaCl structure for the EuTe phase, and (iii) cubic Ge phase.

The homogeneity of our $\text{Ge}_{1-x}\text{Eu}_x\text{Te}$ crystals was studied with the use of the Hitachi SU-70 Analytical UHR FE-SEM scanning electron microscope (SEM) coupled with Thermo Fisher NSS energy dispersive X-ray spectrometer system (EDS) equipped with SDD-type detector. We measured a series of high resolution SEM images of the polished and cleaned crystal surfaces at different sample spots and magnifications. The SEM results

show the presence of micrometer-size inhomogeneities in all our $\text{Ge}_{1-x}\text{Eu}_x\text{Te}$ samples (example in Fig. 2).

The SEM/EDS results reveal the presence of $\text{Ge}_{1-x}\text{Eu}_x\text{Te}$ inhomogeneities in all our samples. These inhomogeneities have the EuTe lattice structure and the chemical composition much higher than the average x value. We also observed the presence of Ge clusters, randomly distributed in the host lattice. EDS spectra taken from several surface areas of the $\text{Ge}_{1-x}\text{Eu}_x\text{Te}$ sample indicate the presence of a small Eu content (maximum of about $x \approx 0.003$), randomly distributed in the semiconductor host lattice.

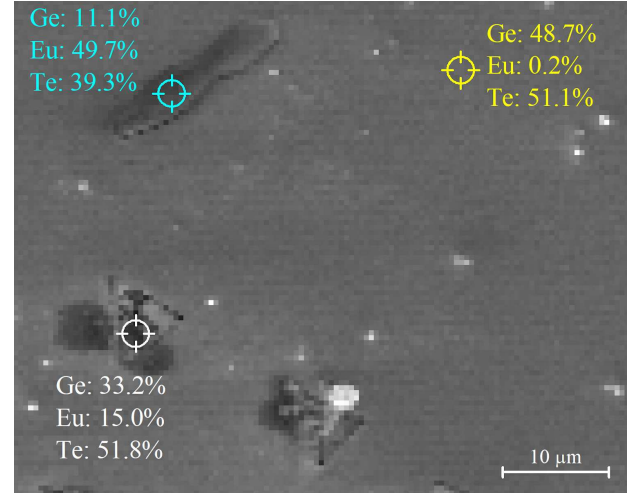


Fig. 2. Selected SEM/EDS results obtained for the $\text{Ge}_{1-x}\text{Eu}_x\text{Te}$ sample with $x = 0.023$ including: SEM image of the sample surface and the calculated chemical compositions measured at the selected spots of the sample surface using the EDS technique.

The electrical properties of our $\text{Ge}_{1-x}\text{Eu}_x\text{Te}$ samples were studied with the use of standard 6-contact Hall geometry magnetotransport measurements at $T = 300$ K and $B < 1.5$ T. The results of the electrical characterization obtained at room temperature are presented in Table I. The carrier mobility increases with the average Eu content, while the carrier concentration seems to be almost constant in our samples. Therefore, it is highly probable that the defect creation in $\text{Ge}_{1-x}\text{Eu}_x\text{Te}$ is a decreasing function of the average Eu content. It should be noted that the transport parameters are average over the whole sample.

TABLE I

Selected parameters obtained from the studies of the $\text{Ge}_{1-x}\text{Eu}_x\text{Te}$ samples with different chemical compositions, x , including: the carrier concentration n , the carrier mobility μ , the Néel temperature T_N , the Curie-Weiss temperature θ , the Curie constant C , the host lattice susceptibility χ_{dia} , the effective Eu content x_θ determined from Eq. (2), the magnetization value M_S at 9 T, and the effective Eu content x_m determined from Eq. (3).

x	n (10^{20}) [cm^{-3}]	μ [$\text{cm}^2/(\text{V s})$]	T_N [K]	θ [K]	C (10^{-4}) [emu K/g]	χ_{dia} (10^{-7}) [emu/g]	x_θ	M_S [emu/g]	x_m
0.020 ± 0.002	7.2 ± 0.2	2.1 ± 0.1	11.1 ± 0.2	-21.6 ± 0.3	7.8 ± 0.7	-2.4 ± 0.1	0.020 ± 0.002	2.7 ± 0.1	0.014 ± 0.001
0.023 ± 0.002	7.1 ± 0.2	33 ± 1	11.2 ± 0.2	-18.2 ± 0.3	9.7 ± 0.9	-2.6 ± 0.1	0.025 ± 0.002	3.1 ± 0.1	0.016 ± 0.001
0.025 ± 0.002	6.6 ± 0.2	44 ± 1	11.1 ± 0.2	-11.2 ± 0.2	11.7 ± 1.1	-2.7 ± 0.1	0.030 ± 0.003	3.4 ± 0.1	0.018 ± 0.001

4. Magnetic properties

Magnetic properties of our $\text{Ge}_{1-x}\text{Eu}_x\text{Te}$ samples were measured with the use of Lake Shore 7229 magnetometer allowing the dynamic magnetic susceptibility χ_{AC} (mutual inductance technique) and the static magnetization M (Weiss extraction technique) measurements.

We performed measurements of the AC magnetic susceptibility over the temperature range from $T = 4.3$ K up to 320 K. The magnetic susceptibility measurements were made with the sample excited by the alternating magnetic field with the frequency, f , equal to 625 Hz and the amplitude, $B_{AC} = 1$ mT. As a result we obtained temperature dependences of real and imaginary parts of the AC magnetic susceptibility, $\text{Re}(\chi_{AC})$ and $\text{Im}(\chi_{AC})$, respectively. The results of the magnetic susceptibility measurements are presented in Fig. 3.

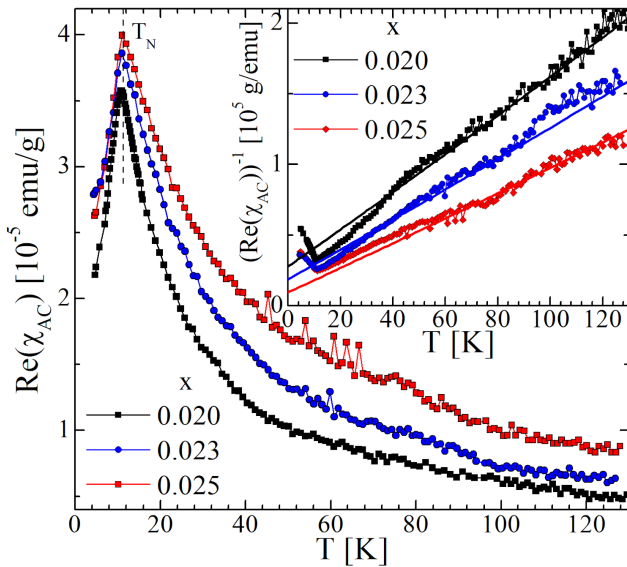


Fig. 3. Temperature dependence of the real part of the AC magnetic susceptibility obtained for $\text{Ge}_{1-x}\text{Eu}_x\text{Te}$ samples with different chemical contents. The inset shows the inverse of the real part of the AC magnetic susceptibility as a function of temperature (points) and fits (lines) of the experimental data to the Curie–Weiss law (Eqs. (1) and (2)).

The $\text{Im}(\chi_{AC})$ dependences for all our $\text{Ge}_{1-x}\text{Eu}_x\text{Te}$ samples were not exceeding 5% of $\text{Re}(\chi_{AC})$. In Fig. 3 we can observe in all our samples the presence of a well-defined magnetic transition at about 11 K. This transition, taking into account the presence of spinodal decompositions with high Eu content, is most probably the paramagnet–antiferromagnet phase transition known for EuTe [10]. The Néel temperature, T_N , estimated for our samples equals to 11 K, a value slightly higher than that for EuTe, where $T_N = 9.58$ K [10]. It is therefore highly probable that the $\text{Ge}_{1-x}\text{Eu}_x\text{Te}$ spinodal decompositions with $0.15 < x < 0.35$ show antiferromagnetism due to superexchange magnetic interactions. The superexchange via an anion is a dominant exchange mechanism

in EuTe [11] and other IV–VI DMS [12]. The estimations are based on the Anderson theory of the superexchange interaction [13]. At $T > 20$ K all our samples behave like Curie–Weiss paramagnetic materials.

The $\text{Re}(\chi_{AC})(T)$ dependence at $T \gg T_N$ for our samples can be described using the modified Curie–Weiss law expressed with the following equation:

$$\text{Re}(\chi_{AC}) = \frac{C}{T - \theta} + \chi_{\text{dia}}, \quad (1)$$

where θ is the Curie–Weiss temperature, and C is the Curie constant described with the following equation:

$$C = \frac{N_0 g^2 \mu_B^2 J(J+1) x_\theta}{3k_B}, \quad (2)$$

where N_0 is the number of cation sites per gram, g is the effective spin splitting factor (for Eu ions $g = 1.993 \pm 0.006$ [11]), J is the total magnetic momentum of Eu ion (for Eu^{2+} we assumed $J = S = 7/2$), μ_B is the Bohr magneton, x_θ is the content of the magnetically active Eu ions, k_B is the Boltzmann constant, and χ_{dia} is the diamagnetic susceptibility of the host lattice. For GeTe $\chi_{\text{dia}} = -3 \times 10^{-7}$ emu/g [14]. The structural characterization of our material, presented above, has shown that our host lattice is not perfect GeTe but consists of different regions. Therefore, we fitted the experimental $\text{Re}(\chi_{AC})(T)$ curves gathered in Fig. 3 to Eq. (1) with three fitting parameters: θ , C , and χ_{dia} . The fits were done in the temperature range from 80 to 320 K and the results can be seen in the inset to Fig. 3. The fitted parameter values are gathered in Table I. The obtained θ values are negative; the absolute values decrease with increase of x . It is a signature of antiferromagnetic interactions in the system. The obtained C values increase as a function of x and allow us to calculate the effective Eu content, x_θ , using Eq. (2). We can see that $x_\theta \geq x$ for all our samples but the values agree within the estimated uncertainty.

We performed the measurements of the magnetization as a function of the magnetic field at several stabilized temperatures below $T = 200$ K in the magnetic field range up to 9 T. The selected $M(B)$ curves obtained for the samples with different chemical compositions, x , at $T = 4.5$ K are presented in Fig. 4.

As we can see in Fig. 4 the magnetization curves obtained at $T = 4.5$ K for all our samples show nonsaturating behavior up to 9 T. The linear increase of the $M(B)$ curves in the magnetic field range up to about 7 T is similar to that observed for EuTe [15] and for $\text{Sn}_{1-x}\text{Eu}_x\text{Te}$ [16], where it was related to the presence of EuTe clusters. Therefore, we suppose that the observed $M(B)$ behavior is related to the presence of $\text{Ge}_{1-x}\text{Eu}_x\text{Te}$ spinodal decompositions. We did not observe the presence of $M(B)$ hysteresis loops (see the inset to Fig. 4) for any of our samples.

We used the highest observed magnetization value at 9 T in order to estimate the effective Eu content, x_m , using the following equation:

$$M_S = x_m N_0 \mu_B g S, \quad (3)$$

where M_S is the magnetization saturation value. The obtained x_m values are, in contrast to the x_θ values, smaller than x . They are underestimated because of the lack of the magnetic saturation.

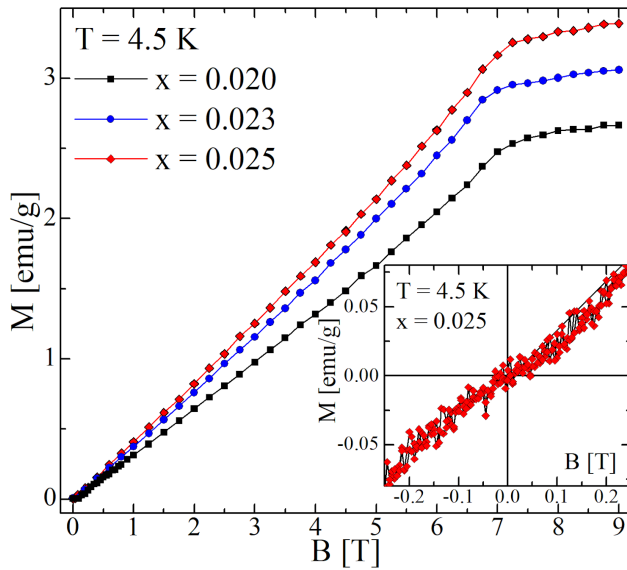


Fig. 4. Magnetization as a function of the applied magnetic field obtained at $T = 4.5$ K for the $\text{Ge}_{1-x}\text{Eu}_x\text{Te}$ samples with different chemical contents, x . The inset shows the low-field region of the $M(B)$ dependence for the sample with $x = 0.025$.

4. Summary

We studied the structural, electrical, and magnetic properties of $\text{Ge}_{1-x}\text{Eu}_x\text{Te}$ bulk crystals with chemical compositions, x , changing from 0.020 to 0.025. The structural characterization of our samples indicated the presence of $\text{Ge}_{1-x}\text{Eu}_x\text{Te}$ spinodal decompositions with high Eu content $0.1 < x < 0.5$ and, possibly, the presence of EuTe clusters. These regions in our samples show antiferromagnetism with the Néel temperature, $T_N \approx 11$ K, characteristic of EuTe. The magnetization curves, $M(B)$, show a linear increase, characteristic of EuTe, and a non-saturating behavior. Both magnetic susceptibility and magnetization data are dominated by the component related to the $\text{Ge}_{1-x}\text{Eu}_x\text{Te}$ spinodal decompositions and EuTe clusters.

References

- [1] Y. Fukuma, H. Asada, J. Miyashita, N. Nishimura, T. Koyanagi, *J. Appl. Phys.* **93**, 7667 (2003).
- [2] W.Q. Chen, K.L. Teo, S.T. Lim, M.B.A. Jalil, T.C. Chong, *Appl. Phys. Lett.* **90**, 142514 (2007).
- [3] Y. Fukuma, H. Asada, S. Miyawaki, T. Koyanagi, S. Senba, K. Goto, H. Sato, *Appl. Phys. Lett.* **93**, 252502 (2008).
- [4] R.T. Lechner, G. Springholz, M. Hassan, H. Groiss, R. Kirchschrager, J. Stangl, N. Hrauda, G. Bauer, *Appl. Phys. Lett.* **97**, 023101 (2010).
- [5] Y. Fukuma, H. Asada, N. Moritake, T. Irisa, T. Koyanagi, *Appl. Phys. Lett.* **91**, 092501 (2007).
- [6] L. Kilanski, M. Górska, R. Szymczak, W. Dobrowolski, A. Podgórn, A. Avdonin, V. Domukhovski, V.E. Slynko, E.I. Slynko, *J. Appl. Phys.* **116**, 083904 (2014).
- [7] A. Podgórn, L. Kilanski, W. Dobrowolski, M. Górska, A. Reszka, V. Domukhovski, B.J. Kowalski, B. Brodowska, J.R. Anderson, N.P. Butch, V.E. Slynko, E.I. Slynko, *Acta Phys. Pol. A* **122**, 1012 (2012).
- [8] M. Górska, J.R. Anderson, J.L. Peng, Z. Golacki, *J. Phys. Chem. Solids* **56**, 1253 (1995).
- [9] K.T. Aust, B. Chalmers, *Can. J. Phys.* **36**, 977 (1958).
- [10] P. Schwob, *Phys. Kondens. Materie* **10**, 186 (1969).
- [11] P. Wachter, in: *Handbook on the Physics and Chemistry of Rare Earths*, Eds. K.A. Gschneidner Jr., L. Eyring, North-Holland, Amsterdam 1979, Vol. 2, p. 507.
- [12] M. Górska, J.R. Anderson, G. Kido, S.M. Green, Z. Gołacki, *Phys. Rev. B* **45**, 11702 (1992).
- [13] P.W. Anderson, in: *Magnetism*, Eds. G.T. Rado, H. Suhl, Academic, New York 1963, Vol. 1, p. 25.
- [14] J.E. Lewis, *Phys. Stat. Sol. B* **38**, 131 (1970).
- [15] H. Hori, R. Akimoto, M. Kobayashi, S. Minamoto, M. Furusawa, N.M. Kreines, A. Yamagishi, M. Date, *Physica B* **201**, 438 (1994).
- [16] J.R. Anderson, M. Górska, Y. Oka, J.Y. Jen, I. Mogi, Z. Golacki, *Solid State Commun.* **96**, 11 (1995).